Automatic registration of urban aerial imagery with airborne LiDAR data

ZHANG Yongjun, XIONG Xiaodong, SHEN Xiang

School of Remote Sensing and Information Engineering of Wuhan University, *Wuhan* 430079, *China*

Abstract: This paper presents a new algorithm for the automatic registration of airborne LiDAR data with aerial images using building corner features as registration primitives. First, three-dimensional building outlines are directly extracted from LiDAR points and building corner features which consist of two orthogonal straight lines are obtained by the regularization of three-dimensional building outlines. Straight lines are also extracted from every aerial image. Second, the building corner features are projected onto aerial images and corresponding image corner features are determined using the similarity measures. Lastly, the exterior orientation parameters are refined by bundle adjustment using the corner points of corner features as control points. Iteration strategy is adopted to obtain optimal results. The main advantage of the proposed algorithm is that the three-dimensional building outlines are extracted directly from LiDAR points without transforming LiDAR points into range image or intensity image, and therefore there are no interpolation errors. The experimental results show that the proposed algorithm can obtain more accurate results in comparison with the registration method based on LiDAR intensity image.

Key words: airborne LiDAR, aerial imagery, registration, line, corner

CLC number: P23 **Document code:** A

Citation format: Zhang Y J, Xiong X D and Shen X. 2012. Automatic registration of urban aerial imagery with airborne LiDAR data. Journal of Remote Sensing, 16(3): 579–595

1 INTRODUCTION

Airborne light detection and ranging (LiDAR) is a modern remote sensing technique for fast terrain data acquisition, which plays a significant role in three-dimensional information acquisition of urban areas. The state-of-art airborne LiDAR system can get colorful aerial images in high resolution simultaneously with laser points. The complementary characteristics between laser points and aerial images (Baltsavias, 1999) provide great prospect in road extraction, building detection and reconstruction, and orthophoto generation (Shan & Toth, 2008; Cheng, et al., 2009; Vu, et al., 2009; Liu, et al., 2007). However, aerial images and LiDAR points usually do not fit well due to boresight misalignment. Therefore, registration procedure must be firstly performed in order to facilitate the following operations.

Intensive researches have been conducted for the registration of LiDAR data with digital optical imagery, which can be generalized into three categories.

(1) Registration between digital optical imagery and LiDAR imagery (intensity images or range images) which are generated from LiDAR points interpolation. It can be divided into two categories, which are the region-based registration and the feature-based registration, respectively. Region-based registration is conducted on pixel grey value level by calculating the similarity between two windows at a special size on two images (Zhang, et al., 2008). For example, the mutual information can be used in registration (Mastin, et al., 2009). In feature-based registration, points and straight-lines are the two features used most frequently. Automatic relating a LiDAR point to the corresponding image point is almost impossible due to the great difference in resolution and imaging mechanism of the two datasets. However, in urban areas corresponding feature points such as building corners can be derived from the intersection of two orthogonal building straight-edges extracted in both LiDAR and optical images, and then these corresponding feature points can be used in the registration. For example, Zhong, et al. (2009) obtain building corner points in both LiDAR range images and digital optical images by intersecting the detected orthogonal building edges, then putative corner points are matched between range images and optical images and registration is performed based on these putative points. Straight-lines also can be used in registration directly, for example, Deng, et al. (2007) extract corresponding straight-lines in optical images and terrestrial LiDAR intensity images and conduct registration based on these corresponding straight-lines. The adoption of LiDAR imagery in registration can simplify the procedure by making full use of the mature image registration algorithms, however, registration errors may be large that are caused by

Received: 2011-04-01; **Accepted:** 2011-07-04

Foundation: National Basic Research Program of China (973 Program) (No.2012CB719904); National Natural Science Foundation of China (No.41171292, 41071233)

First author biography: ZHANG Yongjun (1975—), male, Ph.D. , professor, his research interests are digital photogrammetry and remote sensing, computer vision, and multi-sources date integration. E-mail: zhangyj@whu.edu.cn

the interpolation of LiDAR points.

(2) Dense photogrammetric points can be derived from optical image matching, and then the transformation parameters can be calculated with the principle that the distances between photogrammetric points to LiDAR points is minimal (Pothou, et al., 2006). The drawback of this method is that the obtaining of good initial transformation parameters are essential. Additionally, registration accuracy may not be high enough because of the low accuracy of photogrammetric points.

(3) Direct registration between raw LiDAR points and optical images using the extracted putative features. Straight-lines and planner patches are the most commonly used features in this kind of methods. The research of Habib, et al. (2005) presents two methods for the registration of optical imagery and LiDAR points using straight-lines, but human interaction is indispensable for the extraction and matching of conjugate straight-lines. Planer patch such as building roof in stereo optical images can be represented by the space intersection of three pairs of corresponding points, and then stereo optical images can be georeferenced under the condition that the LiDAR points belonging to the roof are coplanar with the obtained planer patch (Habib, et al., 2006). Errors that caused by LiDAR points interpolation or image matching can be avoided in this kind of method, however, the automation of the registration procedure is restricted by the state-of-art low automation level of extracting and matching of corresponding features between optical images and LiDAR points.

According to the above analysis, to solve the registration problem of LiDAR points with aerial images in urban scenes, this paper presents a new algorithm to detect building contours from raw LiDAR points, and then devises an automatic registration method using building corner features derived from building contours. First, building contours are extracted in irregularly spaced LiDAR points directly, and building corner features in LiDAR data (called LiDAR corner features) are extracted in each regularized building contour by combining two connected orthogonal straight-lines together. Second, each LiDAR corner feature is projected onto the related aerial images using coarse exterior orientation parameters (EOPs) of images, and its corresponding image corner features are identified. Lastly, considering traditional photogrammetric bundle adjustment use point primitives, corner points intersected by the two orthogonal straight-lines of corner features are adopted as control points in the bundle block adjustment to obtain refined EOPs. Iteration strategy is adopted to obtain optimal registration results. The experimental results show that the algorithm can obtain better registration results in comparison with traditional registration method using LiDAR intensity image.

2 BUILDING CORNER FEATURES EXTRACTION IN LIDAR POINTS

The building corner features Extraction in LiDAR points is accomplished in two steps:(1) Building contours extraction. (2) Building contours regularization and building corner features extraction. Each building contour is divided into several polylines with each corresponding to a building edge, and then each polyline is refined by calculating a straight-line using its vertexes. Adjustment is necessary to make sure that the connected two straight-lines are orthogonal to each other. Then, building corner features in LiDAR points (also called LiDAR corner features) are extracted by combining two orthogonal straight-lines together.

2.1 Building contours detection in LiDAR points

This paper proposed an algorithm for detecting building contours in irregularly spaced LiDAR points based on their irregular triangulated networks (TIN). Due to the elevation discontinuity of LiDAR points around the building edges after the LiDAR points fall on building facades have been removed, a set of triangles with two long sides are formed at the facades of the building when LiDAR points are triangulated, (Fig. 1). The boundaries among these triangles and roof triangles are building contours.

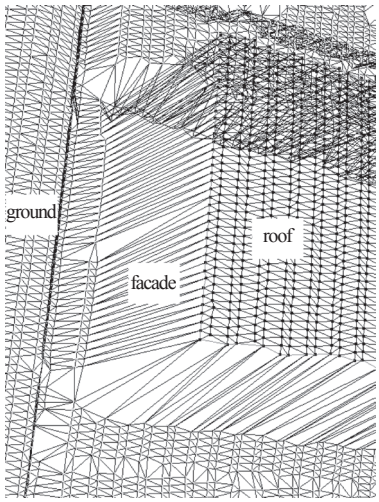

Fig. 1 TIN of building points

A facade triangle with two long sides is shown in Fig. 2, where the vertexes A and B are two adjacent LiDAR points on the edge of building roof. Vertex C is the LiDAR point on ground beside the building, and, ΔZ_{AB}, ΔZ_{AC} and ΔZ_{BC} are the height difference of the three vertexes, respectively (e.g., ΔZ_{AB} is defined as $\Delta Z_{AB}= Z_A - Z_B$, where Z_A and Z_B are the elevations of point A and B, respectively). Considering that the building roof is much higher than ground and the roof is relatively flat at a small area, the following two conditions can be fulfilled for the three vertexes A, B and C.

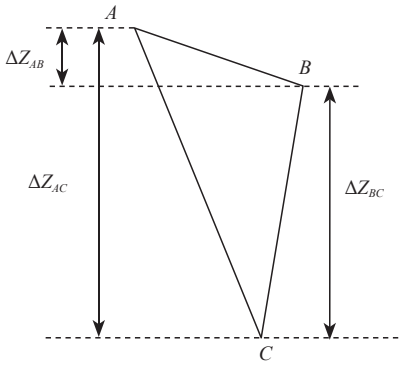

Fig. 2 A sample of Feature triangle

(1) $|\Delta Z_{AB}| < dZ_1$. It means that the two adjacent LiDAR points on building edge should have proximate elevations. And dZ_1 is the maximum tolerance of height difference between two adjacent points on the building edge. Ideally, for buildings with flat roofs, the two adjacent points on building edge should have the same elevation. Considering the vertical precision of LiDAR data, the height difference of the two adjacent points on building edge may not exceed the vertical precision of LiDAR data. Therefore, the value of the threshold dZ_1 is set as the vertical precision of LiDAR data (0.3 m in this paper). For buildings with oblique roofs, in order to extract its oblique edges, a proper larger value of dZ_1 should be calculated according to the LiDAR point space and the obliquity of the roof.

(2) $\Delta Z_{AC} > dZ_2$ and $\Delta Z_{BC} > dZ_2$. It means that building roof should be much higher than ground, where dZ_2 is the minimum tolerance of height difference between building roof and ground. Generally, the height of a building is 3 m at least . Considering that this value may be decreased as affected by the low objects nearby the buildings such as bushes, the value of dZ_2 can be set as 1.5 m.

The above two conditions are called feature triangle conditions. A feature triangle that fills the feature triangle conditions is shown in Fig. 2, where line AB is a feature line-segment. And then the building contour is extracted by connecting the adjacent feature line-segments successively. For the LiDAR data that gained from different LiDAR systems, the value of dZ_1 may be set as the vertical precision of LiDAR data while the value of dZ_2 can be set as 1.5 m at any instance.

Before the extraction of building contours, pretreatment for raw LiDAR points is necessary to remove the outliers and facade points. Outliers can be removed firstly by comparing the elevation of each point with the average elevation of the points within a special range. Then, the remained LiDAR points are divided into several grids, and in each grid points that have height difference with the highest point larger than the threshold ΔH are labeled as facade points and are removed. While the size of the grid can be set as twice as the average point space, the threshold ΔH can be set as the vertical precision of LiDAR data (that is about 0.3 m in this paper).

After the removal of outliers and façade points, LiDAR points are triangulated using two-dimensional Delaunay triangulation strategy and then building contours detection is conducted based on the generated TIN.

The detailed procedures of how to extract building contours from irregularly spaced LiDAR points based on TIN is described as below.

(1) Examine each active triangle (all triangles in TIN are set as active before the procedures) using the feature triangle conditions until a feature triangle is found, and set this feature triangle as current-triangle. Assume the feature line-segment in this feature triangle is AB, where A and B are the two endpoints of line-segment AB, set point A as current-point, and store points B and A as vertexes of a building contour successively.

(2) Examine all the feature triangles that contain current-point besides the current-triangle, and sum up all the feature triangles that contain feature line-segments which has the current-point as an endpoint. ① When the sum of these feature triangles equals to one, assume the feature line-segment in this only one feature triangle is AA_1. Set this feature triangle as current-triangle, and set point A_1 as current-point. If the current-point is the first vertex of this contour line, i.e., A_1 is B, the whole contour line is extracted. Then, go to Step (3). Otherwise, store point A_1 as one vertex of building contour line, and perform another iteration process starting from Step (2) again. ② When the sum of these feature triangles is not one, the contour line is broken here, then go to Step (3).

(3) If the whole contour line is extracted and the number of its vertexes exceeds the given threshold N, store the contour line and go to Step (4). Otherwise, go to Step (4) without storing the contour line. If the extracted contour line is broken, set the first vertex B as current-point and the first triangle as current-triangle, and go to Step (2). Find new vertexes in the opposite direction and insert them at the front of the vertexes sequence of contour line until Step (2) is terminated. Then, store the contour line and go to Step (4) if the number of the vertexes exceeds the threshold N. Otherwise, go to Step (4) directly.

During Step (1) to Step (3), each examined triangle is set as inactive.

(4) The Steps (1), (2) and (3) are repeated until all the triangles are inactive. Then a serial of building contours are extracted.

2.2 Building contour regularization and corner features extraction

Large amount of three-dimensional building contours can be extracted from LiDAR points in urban scenes using the above contours detection algorithm. The segmentation and regularization of each building contour are necessary. Orthogonalization for the two adjacent edges at the building corner is essential, since most buildings have regular shapes and the building corner features are extracted from these buildings.

First, key points of a building contour are decided according to the Douglas-Peucker algorithm, and the building contour is split into several child contours using the key points. Second, each child contour is regularized using the least squares solution. Lastly, the Cluster and Adjustment Algorithm (Shen, et al., 2008) is adopted to re-regularize the child contours by constraining the regularized building edges to the building's dominant directions. All the three-dimensional building contours are projected vertically onto ground during the segmentation and regularization procedures, i.e., only the planimetric coordinates are used. After applying the Cluster and Adjustment Algorithm to child contours, regularized two-dimensional building contours are extracted. Then, regularized three-dimensional building contour straight-lines can be extracted when the elevation of the endpoints of two-dimensional building contour straight-lines are assigned with the elevation of the endpoints of the corresponding child contour lines. The contours of buildings with gable roof can also be extracted when proper value of dZ_1 is set. However, the projection of the two adjacent oblique three-dimensional edges may be parallel to each other on ground, so they may not be distinguished as two edges in the above procedures. To solve this problem, the height difference between each point on child contour and its projected point on the corresponding three-dimensional straight-edge is calculated. If the maximal height difference exceeds a threshold (which can be set as 3 times of the vertical precision of LiDAR data), the three-dimensional

straight-edge should be spilt into two edges at the point with the maximum height difference and re-regularized into two three-dimensional straight-edges.

For each regularized three-dimensional building contour obtained in the above procedures, its both two adjacent straight-lines (e.g., *AB* and *CD*) are checked when their lengths are both larger than a certain value (consider the size of buildings, this value can be set as 3.0 m). If *AB* and *CD* intersect orthogonally at point *F* when projected onto ground and the height difference between the adjacent points *B* and *C* is less than the vertical precision of LiDAR data, straight line-segments *AF* and *FD* are extracted to form a corner feature *AFD*, and the point *F* is called the corner point of this corner feature. The elevation of point *F* is set as the average elevation of *B* and *C*. The corner feature extracted in LiDAR data is called LiDAR corner feature. A series of LiDAR corner features can be extracted when all regularized three-dimensional building contours are processed.

3 SIMILARITY MEASURES OF CORNER FEATURES

The matching of conjugate corner features is described in this section. Each LiDAR corner feature is projected onto related aerial images using the coarse EOPs of the images, as shown in Fig. 3. The polyline *ABC* is a projected corner feature while other straight line-segments and sides of rectangles are extracted straight line-segments in the optical image. First, a circle is drawn around the corner point (the point *B* in Fig. 3) of projected corner feature with a radius of threshold *r*. Second, the straight line-segments that intersect with the circle are selected as candidate straight line-segments. Finally, the corresponding straight line-segments *A′B′* and *B′C′* of the two straight line-segments *AB* and *BC* of projected corner feature are then identified respectively from the candidate straight line-segments using the similarity measurements. And the two selected image straight line-segments *A′B′* and *B′C′* form the corresponding image corner feature *A′B′C′*.

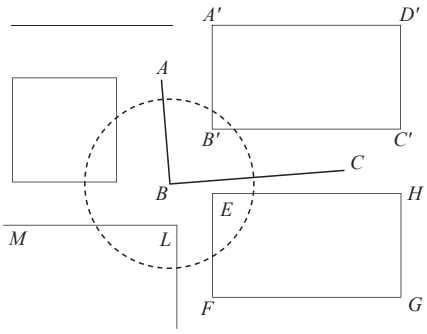

Fig. 3 Matching of conjugate corner features

The main similarity measurement used in conjugate straight line-segments matching is the distance between two straight line-segments. The definition of the distance between two straight line-segments is shown in Fig. 4. *AB* is the LiDAR line-segment that projected onto the image, and *A′B′* is the extracted image line-segment. The distance from point *A′* to the straight line-segment *AB* is d_1, while the distance from point *B′* to the straight line-segment AB is d_2 . And the distance from *A′B′* to *AB* is

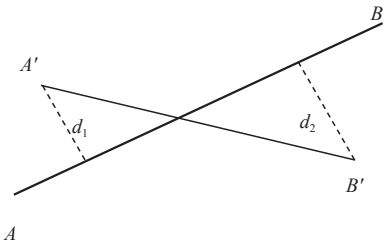

Fig. 4 Distance between two straight line-segments

$$d=(d_1+d_2)/2 \quad (1)$$

Additionally, the length ratio of two straight line-segments and the orientation measurement are also adopted as the similarity measurements in conjugate straight line-segments matching. Ideally, the two conjugate straight line-segments should have the same length; however, the building straight-edges in both aerial images and LiDAR data may not be completely extracted. So in this paper the length ratio of conjugate straight-lines is constrained within 0.5 to 2. The orientation measurement means that the two vectors that represent the conjugate straight line-segments should have the same orientation. As shown in Fig. 3, for the two straight line-segments *BA* and *BC* of the projected corner feature *ABC*, we define point *B* is the origin while point *A* and point *C* are the ends of the two straight line-segments *BA* and *BC*, respectively. And then two vectors *AB* and *BC* formed from the origin to the end are the two vectors that represent the two straight line-segments *BA* and *BC*, respectively. Similarly, for each candidate straight line-segment, the endpoint closer to point *B* is set as the origin (e.g., the point *B′* of the line-segment *A′B′*) while the another endpoint is set as the end (e.g., the point *A′* of the line-segment *A′B′*), and a vector *B′A′* from the origin to the end is also formed to represent the candidate straight line-segment. The intersection angle of two vectors (*BA* and *B′A′*) that represent the two conjugate straight line-segments should be less than 90°.

Two nearest straight line-segments with their two vectors on the same orientation and length ratios between 0.5 and 2.0 will be selected as conjugate straight line-segments. In order to avoid matching outliers, a distance threshold Δd that constrains the distance of conjugate straight line-segments is used. Only if the distance between the conjugate straight line-segments is smaller than Δd, these two conjugate straight line-segments can be valid. Otherwise, the matching result is invalid. The proper values of the two thresholds *r* and Δd should be set according to the accuracy of the coarse EOPs of aerial images, and to make sure that the true conjugate corner features can satisfy the initial value of the two thresholds. Specifically, points belonging to a building roof selected in LiDAR data are projected onto images to evaluate the accuracy of the coarse EOPs.

The matching results may be affected by the fact that some buildings with similar shapes usually are close to each other in the images (e.g., the two adjacent buildings *A′B′C′D′* and *EFGH* shown in Fig. 3). For the straight line-segment BC of the corner feature *ABC*, if only the distance of the straight line-segments and the length ratio are adopted as similarity measurements, there are maybe three matching results (that is *B′C′*, *EH* and

ML, and *B′C′* is the true corresponding straight line-segment). And *ML* can be removed by using the orientation measurements. Due to the low accuracy of the initial EOPs, the first matching result of straight line-segment *BC* may be *EH* or even be *FG* if the EOPs' accuracy is worse, so the corresponding image corner feature may be wrong. However, iteration method with variable weights is adopted in the bundle block adjustment to calculate new EOPs. So more precise EOPs can be obtained provided that most matching results are correct. Then, several iterations are performed, and in each iteration process the EOPs obtained in the previous iteration are used as the initial EOPs. When each iteration process is conducted, the projected corner features will be closer to their true corresponding image corner features. Wrong matching results can be removed gradually by reducing the values of the threshold r and Δd after each iteration until they reach the given minimum value $r_{\min}$ and $\Delta d_{\min}$, respectively. The value of $r_{\min}$ can be set as half of the length of the shortest straight line-segment extracted in aerial images (that is 12 pixels in this paper). The value of $\Delta d_{\min}$ corresponds with the regularization error of the building edges extracted in LiDAR points. In this paper, the regularization error of building edges in LiDAR points is less than half of the point space (about 0.5 m in this paper). Considering the horizontal system error of the LiDAR points (about 0.5 m in this paper), the value of $\Delta d_{\min}$ can be set as the ratio of the sum of the horizontal system error and half of the point space to the ground resolution of aerial images (in this paper the value of $\Delta d_{\min}$ is about 7 pixels). Optimal matching results of the corner features will be obtained after several iterations.

4 AUTOMATIC PRECISE REGISTRATION BASED ON BUILDING CORNER FEATURES

An automatic algorithm for the registration of LiDAR points with aerial images is proposed in this section based on the corner features extraction and matching method presented in the previous sections. As shown in Fig. 5, the algorithm consists of the following steps.

(1) Features extraction. Straight line-segments in aerial images are detected using Canny operator and Hough transformation, while building corner features in LiDAR data can be extracted using the method introduced in Section 2.

(2) Corner features matching. The corresponding image corner features of each LiDAR corner feature are determined using the similarity measurements presented in Section 3 by projecting the LiDAR corner feature onto all related images using the current image EOPs.

(3) Since traditional photogrammetric bundle adjustment uses point primitives, the corner points of conjugate corner features are adopted as control points in the bundle block adjustment of aerial images. The corner point of a corner feature is derived by the intersecting of its two straight line-segments. The corner points obtained in LiDAR data are called LiDAR corner points while the corner points obtained in images are called image corner points. The LiDAR corner points that have corresponding image corner points in more than one images are selected as ground control points (GCPs) in the bundle block adjustment of images, and then refined image EOPs are obtained.

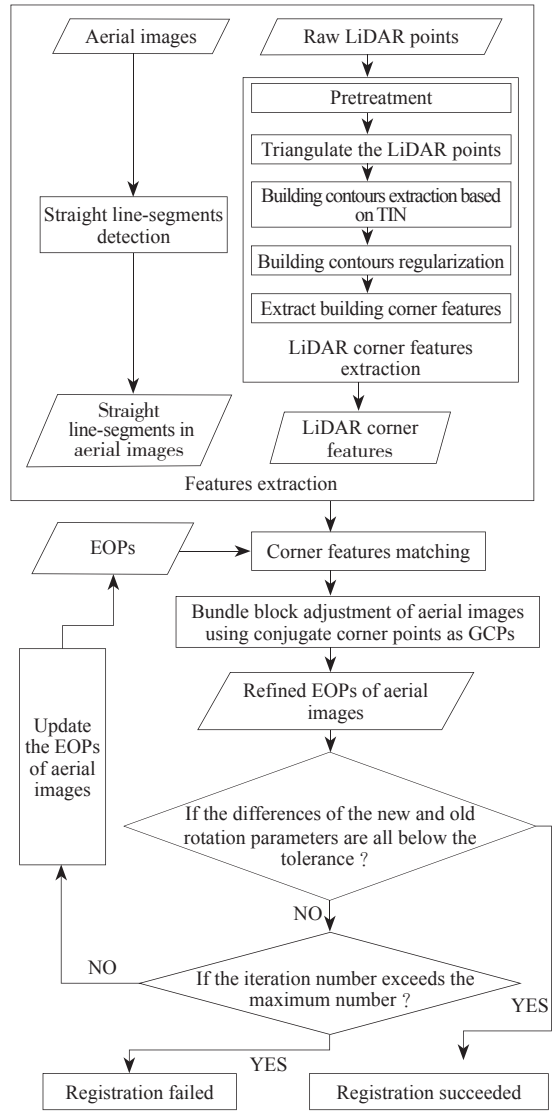

Fig. 5 Flowchart of the registration process

(4) Check whether the iteration process should be continued or not. There are two criteria can be used as the termination of the iterations. The first one is the maximum number of iterations (e.g. 10 times), and the other is the tolerance of difference of the rotation parameters obtained in the prior and current iteration processes (e.g. $1.0e^{-6}$ radians). Iterations from Step (2) to Step (4) will be continued until the iteration numbers exceeds the maximum number or the absolute value of all the differences of rotation parameters are below $1.0e^{-6}$ radians, and in each iteration process the new EOPs obtained in previous iteration are used as the current EOPs. Registration is successful if the iteration number is within the maximum number when the iteration process is terminated.

5 EXPERIMENTS AND RESULTS ANALYSIS

Eight aerial images and corresponding LiDAR data covering an urban area with dense buildings are used to evaluate the proposed registration algorithm. Each aerial image that has a size of 5412×7216 pixels is obtained 950 m above the ground with a

ground resolution at about 0.14 m, while the size of each pixel on the CCD of the camera is 0.0068 mm × 0.0068 mm. The focal length of the camera is 47.323 mm. Fig. 6 shows the planar positions of the aerial images, where 1001—2004 are the IDs of the 8 images in two strips, and A_1—A_9 are the 9 check points manually measured in this area. The average point space of the airborne LiDAR data is about 1.0 m, and the horizontal and vertical precision for the LiDAR data are about 0.5 m and 0.3 m, respectively. The LiDAR data are obtained with the Trimble H56 system in 2010.

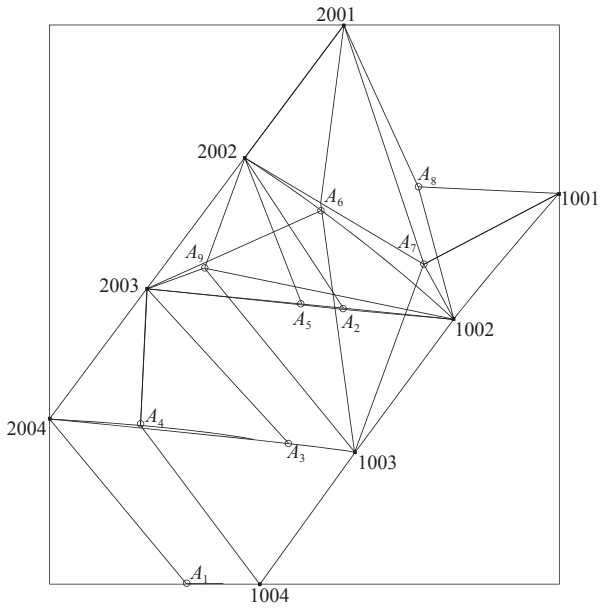

Fig. 6 Planar positions of aerial images

Fig. 7 shows the extracted building contours and regularized contour straight line-segments of two buildings, in which the grey value of the LiDAR points is inversely proportion to their elevation.

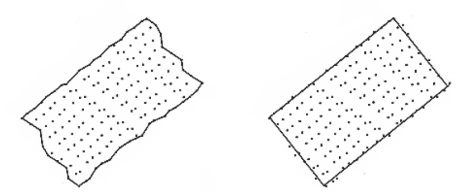

(a) Rectangular building

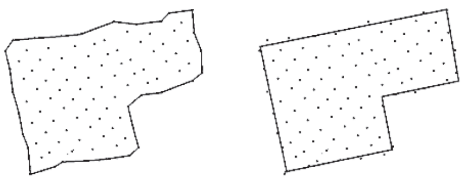

(b) Complex building

Fig. 7 Extracted building contours and LiDAR corner features

Two groups of pictures are demonstrated in Fig. 7, and the left picture of each group demonstrates the extracted building contour with black polylines while the right one demonstrates the regularized building corner features (consists of two connected straight line-segments in the figure). Fig. 7 shows that the proposed building corner features extraction algorithm works well for both the rectangular building Fig. (a) and the complex building Fig. (b).

Considering the large point space of the LiDAR points, the LiDAR points on the extracted building contours are not the actual points that just fall on the building edges. So the regularized building straight edges may have a deviation from their true positions (usually the deviation is less than half of the point space, i.e. about 0.5 m in this paper). The obtained building corner features and their corner points may also have a certain deviation from their true positions. Similar problem also exists in derived GCPs. However, the impact of this deviation can be alleviated by two factors. On one hand, the extracted building corner features and the derived corner points all have shifts to the center of the corresponding buildings. But generally, a lot of corner points will be extracted from each one building, and they usually have opposite orientation of deviations. Therefore, the impact of their deviations to the georefferencing of images can be alleviated in the bundle block adjustment. On the other hand, since the derived GCPs are inaccurate due to the regularization errors (less than half of the point space) and horizontal errors of LiDAR system, the GCPs are treated to be weighted observations in the bundle block adjustment. The horizontal precision of the GCPs can be set as the sum of horizontal precision of LiDAR system (about 0.5 m in this paper) and half of the point space (1.0 m in this paper). The vertical precision of the GCPs can be set as the vertical precision of LiDAR system (0.3 m in this paper). The impact of the inaccurate GCPs to the georefferencing of images can also be alleviated by the weighted strategy.

There are 8422 building corner features extracted in two overlapped strips of LiDAR data, and 902 of them can find corresponding image corner features in more than one image, i.e., 902 GCPs are derived between the LiDAR points and the aerial images. The corresponding image points of the derived GCPs in each image are demonstrated in Fig. 8, where the rectangles represent aerial images and the crosses represent image points of GCPs.

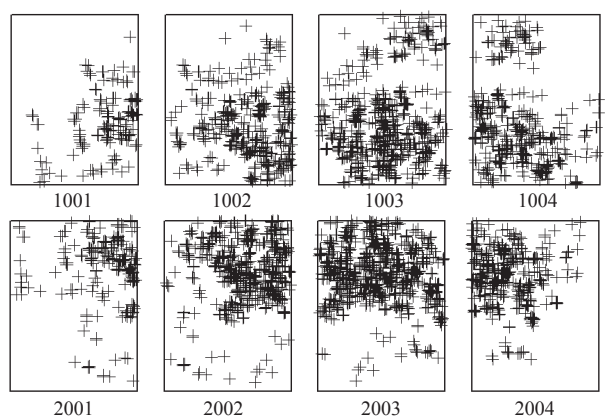

Fig. 8 Distribution of GCPs in aerial images

A GCP that have corresponding image points in five images is shown in Fig. 9, where the cross in the center of Fig. 9 (a), Fig. 9 (b), Fig. 9 (c), Fig. 9 (d) and Fig. 9 (e) indicate its image points in the five images respectively.

Since state-of-art registration of optical images and LiDAR points is mainly realized by conducting registration between optical images and LiDAR intensity images, registration experiment using LiDAR intensity images is also performed to compare with the proposed registration method. In this paper, the LiDAR intensity images and range images are interpolated from the TIN of the LiDAR points at a

space of 0.3 m (it is about 1/3 of the LiDAR point space and twice of the ground resolution of aerial images). 75 GCPs are manually measured between the intensity images and aerial images, most of which are building corners and crosses of roads. The elevation values of the GCPs are obtained from the corresponding range images, and bundle block adjustment of aerial images is conducted using these GCPs.

Fig. 10 shows the projected LiDAR roof points of 8 buildings onto the 8 images in Fig. 6 with the IDs from 1001 to 2004 before and after registration. For each group, the white points in the left, middle and right pictures are the projected LiDAR roof points with coarse EOPs (the POS data of each image in this paper), EOPs obtained from registration using LiDAR intensity images and EOPs obtained from registration using the building corner features, respectively. As we can see from Fig. 10, the LiDAR points in the left pictures of each group all have obvious shifts from their true positions while in the middle and the right pictures the fitness is improved greatly, and the fitness in the right pictures is better than that in the right pictures.

The correctness of the obtained EOPs is verified using 9 manually measured check points numbered from A_1 to A_9, respectively. Table 1 presents the root mean square error (RMSE), average (MEAN), maximum (MAX) of the coordinates residues of the 9 check points before and after registration, where dX, dY and dZ are the residual errors of the X, Y and Z coordinate, respectively; dXY is the planimetric residue. As we can see from Table 1 that, before registration, the RMSE and the maximum (Max.) of planimetric residues are 0.96 m and 1.36 m, respectively; and the RMSE and the maximum of vertical residues are 2.15 m and –4.78 m, respectively. After registration using LiDAR intensity images, the RMSE and the maximum of planimetric residues are 0.37 m and 0.55 m, respectively; and the RMSE and the maximum of vertical residues are 0.23 m and –0.49 m, respectively. After registration using building corner features, the RMSE and the maximum of planimetric residues are 0.25 m and 0.44 m, respectively; and the RMSE and the maximum of vertical residues are 0.13 m and 0.24 m, respectively. Considering that the LiDAR points are obtained at 1.0 m point space with around 0.3 m vertical precision, and the ground resolution of aerial images is about 0.14 m, conclusions can be drawn that the proposed registration method is effective and the registration precision is better than the precision obtained in the method using LiDAR intensity images.

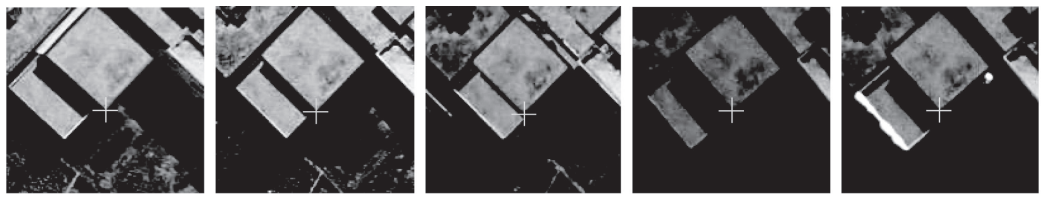

Fig. 9 Five corresponding image points of a GCP

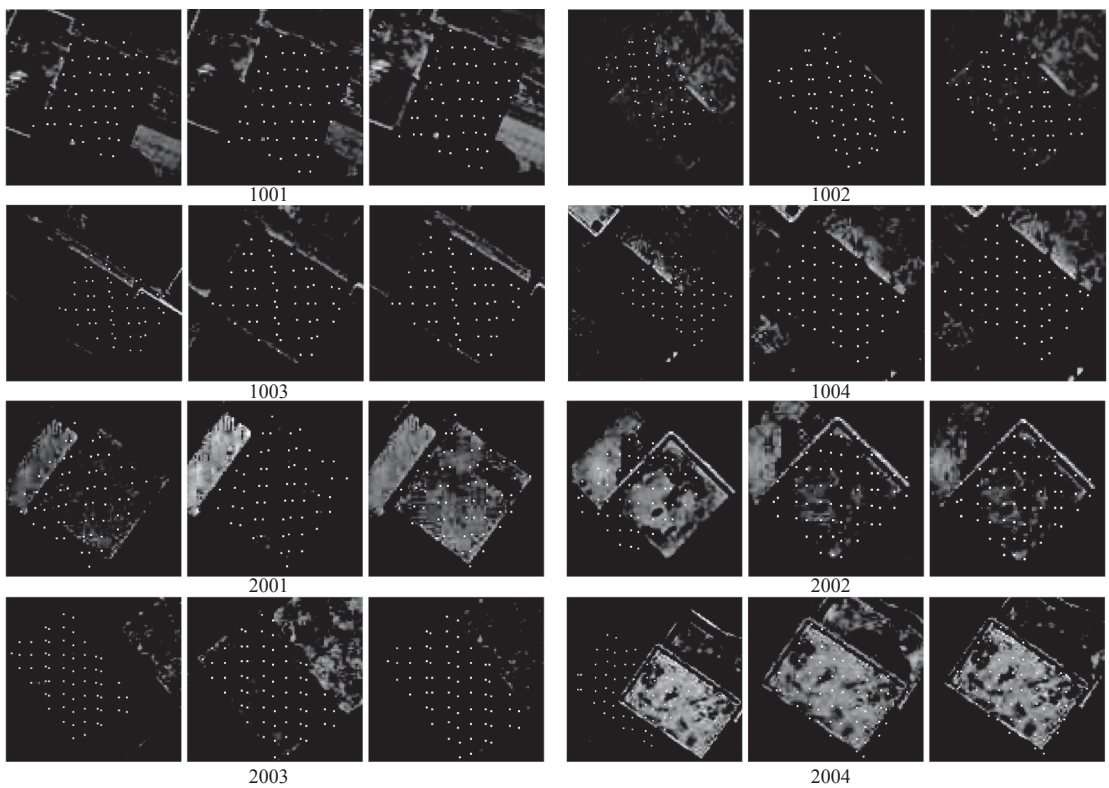

Fig. 10 Comparison of the fitness of roof points to images before and after registration
(For each group, the EOPs used in projection are the coarse EOPs (the POS data of each image), EOPs obtained from registration using LiDAR intensity images and EOPs obtained from registration using the building corner features respectively)

Table 1 Statistics of check points residuals/m

Point name	Before registration				Registration using LiDAR intensity images				Registration using building corner features			
	dX	*dY*	*dXY*	*dZ*	*dX*	*dY*	*dXY*	*dZ*	*dX*	*dY*	*dXY*	*dZ*
A_1	0.38	–0.10	0.39	–2.47	0.05	0.15	0.16	–0.49	–0.07	–0.14	0.16	–0.15
A_2	–1.25	–0.49	1.34	–0.09	0.34	0.06	0.34	–0.11	0.20	–0.06	0.21	0.13
A_3	–0.02	–1.08	1.08	–4.78	0.16	0.06	0.17	–0.12	0.06	–0.12	0.13	0.19
A_4	–0.40	–0.10	0.42	–1.79	0.27	0.24	0.37	–0.29	0.05	0.13	0.14	–0.01
A_5	–1.27	–0.47	1.36	–0.03	0.34	0.16	0.38	–0.20	0.20	0.04	0.20	0.01
A_6	–0.89	0.11	0.89	0.51	0.17	0.27	0.32	–0.21	0.02	0.14	0.14	–0.10
A_7	–0.34	1.02	1.07	2.39	0.28	0.48	0.55	0.03	0.13	0.35	0.37	0.24
A_8	–0.74	0.59	0.95	1.60	–0.15	0.43	0.45	–0.04	–0.32	0.30	0.44	0.08
A_9	–0.58	–0.09	0.59	0.92	0.27	0.30	0.40	–0.14	0.11	0.20	0.23	0.08
RMSE	0.76	0.58	0.96	2.15	0.24	0.28	0.37	0.23	0.16	0.19	0.25	0.13
MEAN	–0.57	–0.07	0.90	–0.42	0.19	0.24	0.35	–0.18	0.04	0.09	0.22	0.05
Max.	–1.27	–1.08	1.36	–4.78	0.34	0.48	0.55	–0.49	-0.32	0.35	0.44	0.24

6 CONCLUSION

To integrate LiDAR points with aerial images in urban scenes, a new automatic registration algorithm using building corner features is proposed in this paper. First, building contours are extracted from triangulated LiDAR points, and LiDAR corner features are obtained from LiDAR date by the regularization of building contours. Second, the corresponding image corner features of each LiDAR corner feature are determined by projecting the LiDAR corner feature onto each aerial image. Finally, the corner points of conjugate corner features between LiDAR data and aerial images are used as GCPs in the bundle block adjustment of aerial images to get refined EOPs. And iteration strategy is adopted to obtain the optimal matching results.

Registration experiments for the method using LiDAR intensity images and the method using building corner features are performed respectively with 8 aerial images and corresponding airborne LiDAR points in an urban area. Then some LiDAR roof points are projected onto aerial images and the residues of 9 check points are calculated to evaluate the performances of the two methods. The results show that our method can acquire satisfying registration results, and the precision is better than that of the method using LiDAR intensity images.

The characters of the proposed method are: (1) The interpolation errors of LiDAR data do not exist because the rasterization procedure is no more necessary; (2) Overall optimal registration results can be obtained by adopting bundle block adjustment even when few GCPs can be extracted in some images provided that the number of GCPs in the whole block is enough; (3) Matching outliers can be removed gradually by using iteration strategy, and optimal registration result can be obtained when the iterations are terminated.

REFERENCES

Baltsavias E P. 1999. A comparison between photogrammetry and laser scanning. ISPRS Journal of Photogrammetry and Remote Sensing, 54(2-3): 83–94

Cheng L, Gong J Y, Li M C, Liu Y X and Song X G. 2009. three-dimensional building model reconstruction from multi-view aerial images and lidar data. Acta Geodaetica et Cartographica Sinica, 38(6): 494–501

Deng F, Zhang Z X and Zhang J Q. 2007. three-dimensional reconstruction of old architecture by laser scanner and digital camera. Science of Surveying and Mapping, 32(2): 29–30

Habib A, Ghanma M, Morgan M and Al-Ruzouq R. 2005. Photogrammetric and lidar data registration using linear features. Photogrammetric Engineering and Remote Sensing, 71(6): 699–707

Habib A F, Shin S, Kim C and Al-Durgham M. 2006. Integration of photogrammetric and LIDAR data in a multi-primitive triangulation environment. [DOI 10.1007/978-3-540-36998-1_3]

Liu X Y, Zhang Z Y, Peterson J and Chandra S. 2007. Lidar-derived high quality ground control information and DEM for image orthorectification. GeoInformatica, 11(1): 37–53

Mastin A, Kepner J and Fisher J. 2009. Automatic registration of lidar and optical images of urban scenes. 2009 IEEE Computer Society Conference on Computer Vision and Pattern Recognition Workshops. Miami Beach: IEEE: 2639–2646

Pothou A, Karamitsos S, Georgopoulos A and Kotsis I. 2006. Assessment and comparison of registration algorithms between aerial images and laser point clouds. Revue Francaise de Photogrammetrie et de Teledetection, (182): 28–33

Shan J and Toth C K. 2008. Topographic Laser Ranging and Scanning: Principles and Processing. Boca Raton: CRC Press: 445–477

Shen W, Li J, Chen Y H, Deng L and Peng G X. 2008. Algorithms study of building boundary extraction and normalization based on lidar data. Journal of Remote Sensing, 12(5): 692–698

Vu T T, Yamazaki F and Matsuoka M. 2009. Multi-scale solution for building extraction from lidar and image data. International Journal of Applied Earth Observation and Geoinformation, 11(4): 281–289

Zhang F, Huang X F and Li D R. 2008. A review of registration of laser scanner data and optical image. Bulletin of Surveying and Mapping, (2): 7–10

Zhong C, Li H, Huang X F and Li D R. 2009. Automatic registration of lidar data and aerial image based on a 6-tuples relaxation. Geomatics and Information Science of Wuhan University, 34(12): 1426–1430

城区机载LiDAR数据与航空影像的自动配准

张永军，熊小东，沈翔

武汉大学 遥感信息工程学院，湖北 武汉 430079

摘 要：为解决机载LiDAR数据与航空影像集成应用中二者的配准问题，提出了一种机载LiDAR数据与航空影像配准的方法。首先，直接在LiDAR点云中提取建筑物3维轮廓线，通过将轮廓线规则化得到由两条相互垂直的直线段组成的建筑物角特征，并在航空影像上提取直线特征；然后，根据影像初始外方位元素将建筑物角特征投影到航空影像上，并采用一定的相似性测度在影像上寻找同名的影像角特征；最后，将角特征的角点当作控制点，利用传统的摄影测量光束法区域网平差解求影像新的外方位元素。解算过程中采用循环迭代策略。本方法的主要特点是，直接从LiDAR点云中提取线特征，避免了常规方法从距离图(或强度图)中提取线特征所产生的内插误差。通过与现有基于点云强度图的配准方法的对比实验表明，在低精度初始外方位元素的辅助下，本文方法能够达到较高的配准精度。

关键词：机载LiDAR，航空影像，配准，线特征，角特征

中图分类号：P23 **文献标志码**：A

引用格式：张永军，熊小东，沈翔. 2012. 城区机载LiDAR数据与航空影像的自动配准. 遥感学报，16(3): 579–595
Zhang Y J, Xiong X D and Shen X. 2012. Automatic registration of urban aerial imagery with airborne LiDAR data. Journal of Remote Sensing, 16(3): 579–595

1 引 言

机载激光探测与测距(机载LiDAR)是一项能够快速获得地形数据的重要技术，目前已成为获取城市3维信息的重要手段。当前的机载LiDAR系统通常配备有数码相机，可在获取激光点云的同时获得高分辨率彩色航空影像。由于激光点云和影像数据之间具有很强的互补性(Baltsavias，1999)，二者的集成在道路提取、建筑物提取与建模以及正射影像制作等领域有着广泛的应用(Shan和Toth，2008；程亮 等，2009；Vu 等，2009；Liu 等，2007)。由于数码相机安置误差等原因，获得的航空影像的外方位元素一般存在较大误差，导致航空影像与激光点云之间无法很好地套合，因此在集成应用二者之前，需要将它们纳入到统一的坐标系中，即进行航空影像与激光点云的配准。

在数码影像与激光点云的配准方面，目前已有大量的研究，现有的配准方法大致可分为3类：

(1)将激光点云内插生成图像(强度图像或距离图像)，然后在点云图像和数码影像之间进行配准。点云图像和数码影像的配准，根据所采用的配准基元，可以分为两类：基于灰度区域的配准和基于特征的配准。基于灰度区域的配准通过比较影像上一定大小窗口中灰度分布的相似程度，在灰度层次上进行配准(张帆 等，2008)，如利用互信息作为相似性测度进行配准(Mastin 等，2009)。基于特征的配准中常用的特征有点特征和线特征。由于激光点云和数码影像在成像方式和分辨率上差异显著，直接在点云图像和影像之间自动地匹配同名点具有相当的难度。在城市地区存在着大量的建筑物轮廓线，可通过提取建筑物直线边缘，然后将相邻且相互垂直的边缘相交获得角点特征用于配准。如钟成等人(2009)分别在机载LiDAR距离图像和航空影像上提取直线边缘，进而交会出建筑物角点，然

收稿日期：2011-04-01；**修订日期**：2011-07-04

基金项目：国家重点基础研究发展计划(973计划) (编号: 2012CB719904)；国家自然科学基金(编号: 41171292，41071233)

第一作者简介：张永军(1975—)，男，教授，博士生导师。主要从事数字摄影测量与遥感、计算机视觉，多源数据融合等方面的研究。E-mail: zhangyj@whu.edu.cn。

后匹配同名角点用于配准。在以直线特征作为配准基元方面，邓非等人(2007)将地面激光点云内插成强度图像，然后在强度图像和数码影像上提取并匹配同名直线段用于配准。点云内插成图像与数码影像进行配准的方法，其优点是可以充分利用目前已十分成熟的图像配准算法，其缺点是在对点云内插的过程中会引入内插误差，影响最终的配准精度。

(2)将数码影像密集匹配为摄影测量点云，然后以两点集之间距离最近为原则计算激光点云和摄影测量点云之间的坐标变换，实现激光点云与影像的配准(Pothou 等，2006)。该类方法需要较好的初值，此外，数码影像密集匹配生成的点云精度一般比较低，会降低配准精度。

(3)直接在激光点云和数码影像之间进行配准。主要是通过在激光点云和数码影像之间寻找同名特征实现配准。常用的特征主要有直线特征和平面特征。Habib等人(2005)的研究给出了直接从点云中提取直线段进行配准的两种可行的方法，不过其在激光点云中提取直线段以及在激光点云和数码影像中匹配同名直线段都需要手动进行。以平面特征作为配准基元时，一般是在立体影像对中人工匹配屋顶等平面上的3对同名点，交会出物方平面，再根据激光点云中属于该平面的点与该平面共面的条件实现影像对的定位(Habib 等，2006)。该类方法的优点是不需要对激光点云进行图像内插或者对影像进行密集匹配，避免了在点云内插或影像密集匹配过程中引入误差，然而此类方法的自动化实现有赖于点云和影像中同名特征的自动提取和匹配，而目前其自动化程度有待提高。

基于上述分析，针对城市地区机载LiDAR数据与航空影像的配准问题，本文提出一种直接从机载LiDAR点云中提取建筑物轮廓线的方法，进而设计了一种以建筑物角特征作为配准基元的自动化配准方案。该方案直接在LiDAR点云中提取建筑物轮廓线，通过对轮廓线规则化得到拟合成直线段的建筑物轮廓边，以两相邻且垂直的轮廓边组合成一个建筑物角特征(称为LiDAR角特征)；然后根据航空影像初始外方位元素将LiDAR角特征投影到影像上，根据一定的相似性测度寻找与其同名的影像角特征；鉴于点在传统摄影测量中的优势性，最后将角特征中两直线段的交点作为控制点进行航空影像的光束法区域网平差，求解影像新的外方位元素。运算中可通过迭代提高配准精度。通过与目前基于点云强度图的配准方法的对比试验表明，本方法能够取得很好的配准效果，且配准精度优于基于点云强度图的配准方法。

2 LiDAR点云中角特征的提取

LiDAR点云中角特征的提取可分为两个步骤：线特征提取—获得建筑物轮廓线；轮廓线规则化与角特征提取—提取轮廓线关键点，用直线段简化轮廓线，并进行转角的直角化，然后将相互垂直的相邻直线段组合成角特征。

2.1 LiDAR点云中线特征的提取

为了从LiDAR点云数据中提取建筑物角特征，首先需要提取建筑物轮廓线这一类特征线。本文提出了一种基于点云不规则三角网(TIN)的点云特征线提取算法。图1为一片包含建筑物的点云所构建的不规则三角网，由于在建筑物的边缘处高程存在突变，在建筑物的墙面处会形成一系列具有两条长边的墙面三角形，在三角网中墙面三角形与屋顶三角形的交界线即为本文要提取的建筑物轮廓线。图2为墙面处一个具有两条长边的墙面三角形示意图，其中顶点A、B分别为建筑物屋顶边缘上的两个相邻的LiDAR点，C为墙脚附近地面上的LiDAR点，ΔZ_{AB}(定义 $\Delta Z_{AB}=Z_A-Z_B$，Z_A和Z_B分别表示点A、B的高程)、ΔZ_{AC}和ΔZ_{BC}分别为3个顶点之间的高程差。由于建筑物屋顶边缘到地面具有一定的高度，而建筑物屋顶一般相对平坦，所以这3个顶点的高程差应满足：(1)$|\Delta Z_{AB}|<dZ_1$，即建筑物边缘上两相邻LiDAR点的高程应该相近，其中dZ_1表示建筑物边缘上两相邻LiDAR点的最大高差，对于平顶建筑物，理论上边缘上两相邻点的高程值应该相等，考虑到LiDAR系统测量点位的高程误差(本文中LiDAR系统测点的高程精度约为0.3 m)，建筑物边缘上两相邻点A、B的高程差不应超过这一高程误差值，故将dZ_1设为LiDAR点云的高程精度，本文中为0.3 m，对于人字形建筑物的倾斜边缘，根据边缘上相邻LiDAR点的平均间距和屋顶倾斜度，适当放宽dZ_1的值，可提取出人字形建筑物的倾斜边缘；(2)$\Delta Z_{AC}>dZ_2$且$\Delta Z_{BC}>dZ_2$，即屋顶边缘上的点与地面点的高程应该存在突变，dZ_2表示屋顶边缘到地面的最小高度差，一般建筑物的高度至少有3.0 m，考虑到建筑物附

近的地面上常会有一些植被等低矮物体，会使得屋顶边缘与地面的高度差有所减少，故本文中将dZ_2设为建筑物最低高度的一半，即1.5 m。上述两个条件称为特征三角形条件，图2所示三角网中符合上述两个条件的三角形称为特征三角形，该三角形中的线段AB即为特征线段，相邻的特征线段依次相连组成本文所要提取的建筑物轮廓线特征。在实际数据处理中，对于不同系统获得的激光点云数据，阈值dZ_1可设置为该点云数据的高程精度，而阈值dZ_2与最低建筑物的高度有关，根据上述分析，可固定设置为1.5 m。

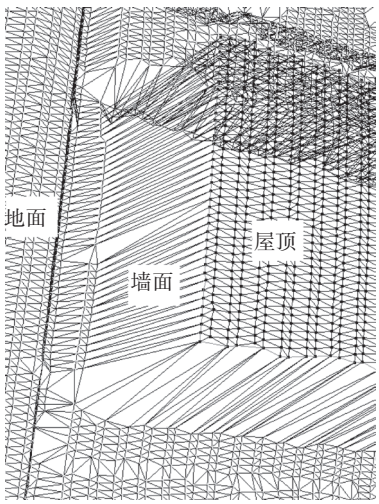

图1 点云TIN局部

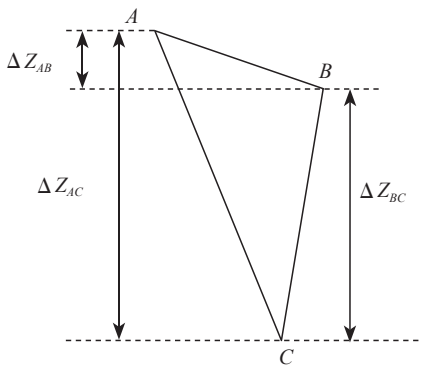

图2 特征三角形示意图

在提取点云中线特征之前，需要对原始点云进行预处理，滤除其中的粗差点和墙面点。粗差去除可通过比较每点与周围其他点的高程平均值的方式进行。墙面点的剔除在去除粗差点之后进行，可对LiDAR点云划分格网，在每个格网内找出高程最大值，然后剔除那些高程值与高程最大值相差大于阈值ΔH的点，ΔH可设置为点云的高程精度(本文中约为0.3 m)，格网间距可取平均LiDAR点间距的2倍。

滤除点云中的墙面点和粗差点后，采用2维Delaunay方法对点云构建不规则三角网，再基于点云不规则三角网提取点云特征线。

基于点云不规则三角网提取点云特征线的算法步骤如下：

步骤 1 遍历三角网中的有效三角形(计算开始时三角网中所有三角形均设置为有效)，直至找到一个满足特征三角形条件的三角形，将其设置为当前三角形。设此三角形中特征线段为AB，其两个端点分别为A和B，将点A设为当前点。依次存储点B、A到线特征的点队列。

步骤 2 在除当前三角形以外的所有以当前点为顶点的三角形中，根据特征三角形判定条件寻找所有包含特征线段、且特征线段的一端点为当前点的特征三角形：(1)如果仅有一个符合条件的三角形，设特征线段为AA_1，将该三角形设置为当前三角形，将点A_1设置为当前点。将当前点与点B比较，如果它们为同一点，则线特征闭合，转到步骤 3，否则存储点A_1，并继续执行步骤 2；(2)如果符合条件的三角形的个数不等于1，则线特征在此处中断，转到步骤 3。

步骤 3 对于闭合的线特征，如果总点数大于阈值，保存该线特征，进入步骤 4，否则直接进入步骤 4；对于未闭合的线特征，则转到步骤 2，以点B为当前点进行反向搜索，将搜索到的线特征点插入队列之前，直至步骤 2执行终止，如果此时线特征上点数大于阈值，保存该未闭合的线特征，进入步骤 4，否则直接进入步骤 4。

在步骤 1—3中，每当一个三角形判断完毕后，就将其设置为无效。

步骤 4 重复步骤 1—3直至所有三角形均已无效，此时得到多条线特征。

2.2 建筑物轮廓线规则化及角特征提取

采用上述点云特征线提取算法，可以在城市点云数据中提取出大量的建筑物轮廓线。然而，所提取的建筑物轮廓一般为锯齿状，且由建筑物多条轮廓边相连而成，因此，需要对轮廓线进行分段，对每一段拟合直线。本文只考虑从具有规则轮廓的建筑物上提取角特征，因此需要对轮廓线的拐角进行直角化。

本文采用Douglas-Peucker算法确定轮廓线的关键点，并根据关键点将轮廓线拆分成多条子轮廓线，然后利用最小二乘法对每一条子轮廓线进行直线段拟合，最后采用分类强制正交法(沈蔚 等，2008)将每一

条子轮廓线重新拟合成分布在建筑物主方向上的直线段。此处在对建筑物轮廓线进行规则化时，将轮廓线垂直投影到地面上，即只考虑轮廓线的2维坐标。在通过“分类强制正交”获得规则化的2维直线段后，直线段端点的高程值取相应子轮廓线端点的高程值，可获得规则化的3维轮廓。当特征三角形条件的阈值dZ_1设置得较大时，也可提取出人字形建筑物的轮廓，由于人字形建筑物的人字形轮廓边投影到地面上为一条直线，经过规则化处理后只能得到一条3维直线，与实际不相符。为了准确提取人字形轮廓边的两条直线边，需要计算子轮廓线上每一点与其在对应的3维直线上的投影点的高程差，找出高差最大的点，如果高差超出阈值(考虑到点云高程误差，可取3倍的点云高程精度)，则用该点与3维直线段的两端点重新拟合出人字形轮廓边的两条直线边。

对于规则化的3维轮廓，依次对相邻直线段进行判断，如果两直线段AB和CD的长度超过设定的阈值(根据建筑物的尺寸，可设定为3 m)且在xy平面上相互垂直，且两邻近端点B和C的高程值差异在点云高程精度内，则计算两直线段在xy平面上的交点F作为建筑物角点，F的高程值取B和C高程平均值。线段AF和FD即组合为一个建筑物角特征AFD(称为LiDAR角特征)。依次对每条3维轮廓线进行处理，可提取出大量的建筑物角特征。

3 角特征的相似性测度

同名角特征的匹配方法如图3所示。根据影像初始外方位元素将LiDAR角特征投影到影像上，得到图中粗折线ABC所示的投影角特征，图中其他的矩形边和线段表示在影像上提取的直线段。首先，以角特征的角点B为中心作一个半径为阈值r的圆(图中虚线所示)；然后，将所有与圆面相交的影像直线段取出作为候选直线段；最后，在候选直线段中，根据直线段的相似性测度分别为角特征的AB和BC两条线段寻找同名直线段$A'B'$和$B'C'$，$A'B'$和$B'C'$组成与LiDAR角特征同名的影像角特征$A'B'C'$。

在进行直线段匹配时，采用直线段之间的距离作为同名直线段匹配的相似性测度。直线段之间的距离的定义如图4所示，AB为投影到影像上的直线段，$A'B'$为影像上提取的直线段，点A'到直线AB的距离为d_1，点B'到直线AB的距离为d_2，则直线段$A'B'$到直线

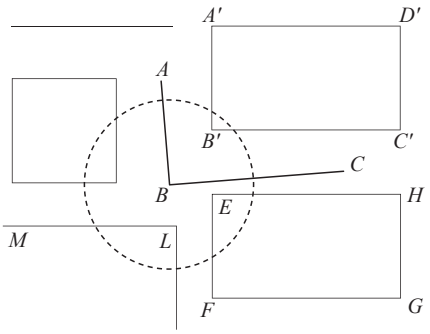

图3 同名角特征匹配示意图

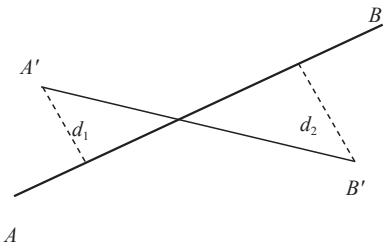

图4 直线段之间的距离示意图

段AB的距离定义为

$$d=(d_1+d_2)/2 \tag{1}$$

此外，还引入直线段长度比和方向测度作为直线段匹配条件。直线段长度比用来限定同名直线段的长度差距，理论上同名直线段应该具有相同的长度，考虑到在LiDAR点云和航空影像上提取的建筑物边缘很可能并不完整，可限定两同名直线段的长度比不能超过2，即应在0.5—2倍。方向测度用来限定同名直线段之间的夹角，在图3中，投影角特征ABC的两条线段BA、BC中，规定B为起点，A、C分别为两线段的终点，从起点到终点构成一个向量(如BA和BC)。在影像上的候选直线段中，离点B近的端点作为起点(如线段$A'B'$中的B')，另一端点作为终点(如线段$A'B'$中的A')，同样也可以构成一个起点到终点的向量$\boldsymbol{B'A'}$。同名直线段的向量方向应该相同(向量$\boldsymbol{BA}$与$\boldsymbol{B'A'}$夹角小于阈值90°)，即方向测度。

同名直线段匹配时，选择长度比小于2、向量方向相同、距离最近的两直线段作为同名直线段，为了尽量避免误匹配，应根据外方位元素的精度设定一个直线段距离阈值Δd。只有满足长度比条件和方向条件，且距离小于阈值Δd的最邻近的两直线段才被认为是同名直线段。在实际运用中，前述选择候选直线段时的圆半径阈值r以及此处的直线段距离阈值Δd均需根据初始的外方位元素的精度来确定，设定的r与Δd的初始值必须保证真实的同名角特征之间能够满足这两个阈值，可在配准前将一片屋顶点云投影到影像上，从而

评定初始方位元素的精度以及设定r与Δd的初始值。

在同名角特征匹配过程中，如果两建筑物非常相似且相邻，如图3中的建筑物$A'B'C'D'$与$EFGH$，在寻找角特征ABC的两直线段BA、BC的同名直线段的过程中，以线段BC为例，仅仅以直线段距离以及直线段长度比为测度，其同名直线段有3种可能的结果，即$B'C'$、EH和ML，再以方向测度作进一步约束，可剔除ML。由于受初始外方位元素精度的影响，线段BC的初次匹配结果很可能是线段EH(当初始外方位元素更差时匹配结果甚至可能是FG)，从而使该角特征匹配获得错误的影像同名点。然而由于本文采用光束法区域网平差，在平差过程中对于所有控制点采用选权迭代法，只要大多数的控制点及其像点是正确的(或者是离正确的位置很近)，即可自动地剔除控制点粗差，获得更准确的影像外方位元素。进而，采用循环迭代策略，将前次配准得到的影像外方位元素当作初始值代入本次配准，每次迭代以后，投影的角特征线段会逐步靠近其真实的同名影像线段，直至最终收敛得到正确的匹配结果。同时，每迭代一次，逐步减小圆半径阈值r和距离阈值Δd直至分别达到设定的最小值$r_{\min}$和$\Delta d_{\min}$，从而逐步缩小匹配的拉入范围并剔除误匹配，$r_{\min}$可设置为在影像上提取的最短直线段长度的一半(本文中约为12个像元)。$\Delta d_{\min}$根据LiDAR点云中建筑物边缘的拟合误差设定，本文在LiDAR点云中建筑物边缘的拟合偏差一般不超过半个LiDAR点间距(本文约为0.5 m)，考虑到LiDAR点的平面精度(本文约为0.5 m)，$\Delta d_{\min}$可设置为半个LiDAR点间距与点云平面精度之和与影像地面分辨率的比值，其在影像上的单位为像元，本文约为7个像元。经过多次迭代后，同名角特征匹配结果的可靠性和精度会达到最优。

4 基于建筑物角特征的高精度自动配准

基于上文对LiDAR点云角特征提取、点云与影像间同名角特征匹配方法的介绍，本文设计了如图5所示的LiDAR数据与航空影像高精度自动配准方案。具体流程如下：

(1)特征提取。在航空影像上提取直线特征，在LiDAR点云中提取建筑物角特征(称为LiDAR角特征)。在航空影像上采用Canny算子和Hough变换提取建筑物边缘等直线特征；对于LiDAR点云数据，通过滤除粗差点及墙面点、构建TIN、提取特征线、规则化特征线及提取建筑物角特征，获得一系列的LiDAR角特征。

(2)匹配同名角特征。对于每一个LiDAR角特征，利用现有的影像外方位元素将它投影到每张影像上，根据角特征的相似性测度，寻找LiDAR角特征在所有影像上同名的影像角特征。

(3)将角特征中两线段的交点作为角特征的角点，以LiDAR角特征的角点作为地面控制点，以其同名影像角特征的角点为该控制点的像点。利用所有两度及以上重叠的控制点对航空影像作光束法区域网平差，获得新的影像外方位元素。

(4)检查计算是否收敛。根据影像新旧外方位元素计算本次迭代中外方位元素的改正数，将角元素改正数与规定的限差比较，一般限差设定为百万分之一弧度。当3个角元素的改正数均小于限差时，迭代收敛，输出当前影像外方位元素作为配准结果；否则，将当前得到的影像外方位元素作为初值，继续执行第(2)、(3)、(4)步，直至迭代收敛或者达到最大迭代次数。

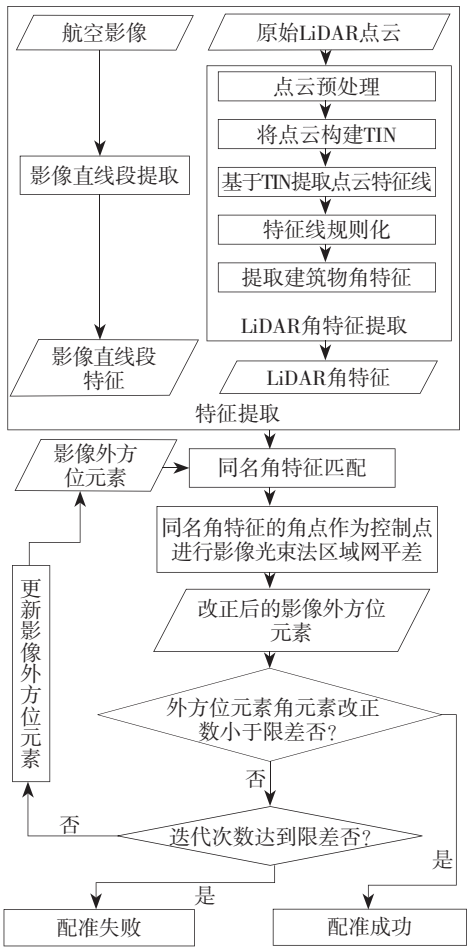

图5 基于建筑物角特征的LiDAR数据与航空影像配准方案

5 试验及结果分析

为验证文中提出的LiDAR数据与航空影像高精度自动配准方法的有效性，本文利用8张航空影像与同一地区的机载LiDAR数据做了配准实验。测区为某城镇，建筑物较密集；航空影像的像幅大小为5412×7216像元，相机的CCD像元大小为0.0068 mm，相机焦距为47.323 mm，航高约为950 m，影像地面分辨率约为0.14 m。图6为测区航空影像分布情况，有1001—2004共8张影像，分为两条航带，A_1—A_9为测区内9个检查点。试验中使用的LiDAR数据是2010年由Trimble H56系统获得的，LiDAR数据的平均点间距约为1.0 m，平面精度约为0.5 m，高程精度约为0.3 m。

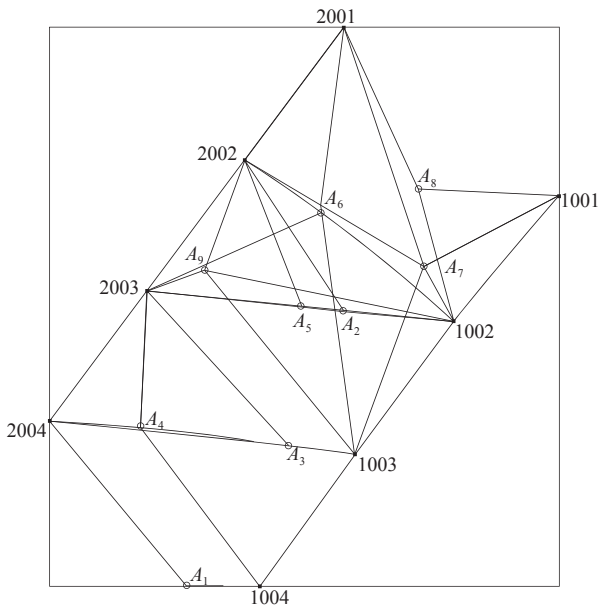

图6 测区内航空影像的分布

图7为从点云数据中提取的线特征以及将线特征规则化后得到的建筑物角特征(LiDAR点按其高程显示为不同的灰度)，共有(a)、(b)两组结果，每一组中左边为提取的轮廓线(黑色的折线所示)，右边为轮廓线规则化后得到的建筑物角特征(黑色的直线段为组成角特征的线段)。其中(a)为针对矩形建筑物的试验结果；(b)为针对多边形建筑物的试验结果。从图中可见，无论对于简单的矩形建筑物还是结构较复杂的多边形建筑物，采用本文的轮廓线提取算法均能得到理想的效果。

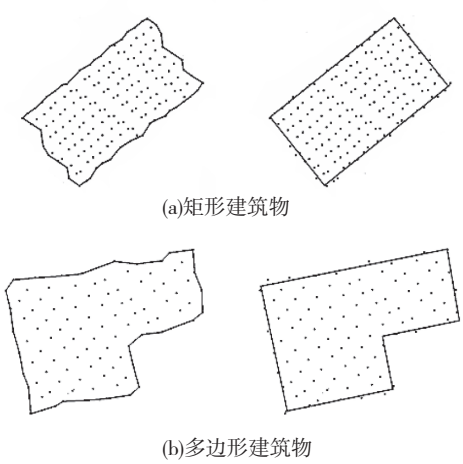

(a)矩形建筑物

(b)多边形建筑物

图7 从点云数据中提取的线特征和角特征

在对轮廓线进行规则化的过程中，对边缘点采用最小二乘的方法拟合建筑物的直线边缘时，考虑到所用的边缘点并非都正好落在屋顶边缘，拟合出的直线位置与实际位置可能存在不超过半个LiDAR点间距的偏差(本文中约为0.5 m)，会使得到的建筑物角特征及角点的几何位置产生一定的偏差，进而使提取的控制点坐标值产生一定的误差。本文中提出的配准方法有两方面的因素可以减弱这种偏差的影响：一方面，提取的角特征的位置与其实际位置相比，都会向建筑物内侧收缩，从而使得最后得到的控制点的位置也会向建筑物内侧收缩，但是由于一般在一栋建筑物上可以提取出多个角点，它们正好朝相反的方向偏移，当进行光束法区域网平差时，所有控制点的偏移造成的影响会在一定程度上得到抵消；另一方面，在光束法平差过程中，根据上述分析得到的控制点偏差值(不超过半个LiDAR点间距)以及LiDAR系统测量的平面精度(本文中使用的LiDAR系统测点的平面精度约为0.5 m)，为控制点设定相应的坐标精度(即权值)，控制点的平面精度应设置为半个LiDAR点间距与LiDAR系统平面精度之和，本文中约为1.0 m，控制点的高程精度应设为LiDAR系统测点的高程精度，本文中约为0.3 m。通过为控制点设定一定的精度，可在区域网平差中获得整体最优解，在一定程度上消除控制点位置偏差的影响。

试验时在两条航带的LiDAR数据(有一定重叠)中共提取8422个LiDAR角特征，最终有902个角特征能够在至少两张上影像上找到同名的影像角特征，即得到902个控制点。图8为所有地面控制点的像点在影像上的分布图，每个矩形框表示一张影像，十字丝表示像点。

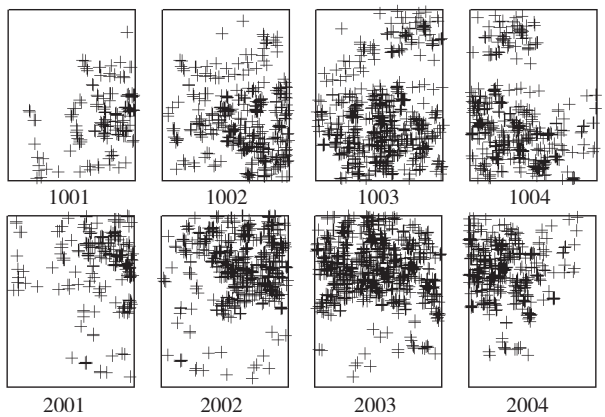

图8 测区内所有控制点在影像上的像点分布

图9为在影像上具有5度重叠的角点控制点图像，其中图9(a)—(e)中间的十字丝分别指示该控制点在5张影像上的像点位置。

由于目前影像与LiDAR点云配准主要是通过将点云内插成强度图，利用强度图与光学影像进行配准，故本文试验了利用强度图进行配准的方法，并与本文基于角特征的配准方法做对比分析。本文以0.3 m的重采样间隔(约为LiDAR点间距的1/3，约为航空影像地面分辨率的2倍)通过三角网内插生成了点云数据的强度图像和距离图像，在强度图上人工量取了75个均匀分布的控制点(主要为建筑物角点和道路交叉点等)以及它们在相关影像上的像点，在相应的距离图像上计算获得控制点的高程值，并采用这些控制点对影像进行光束法区域网平差。图10所示为两种配准方法的对比试验结果，共有8组图片，分别展示了图6中编号为1001—2004 8张影像上的局部

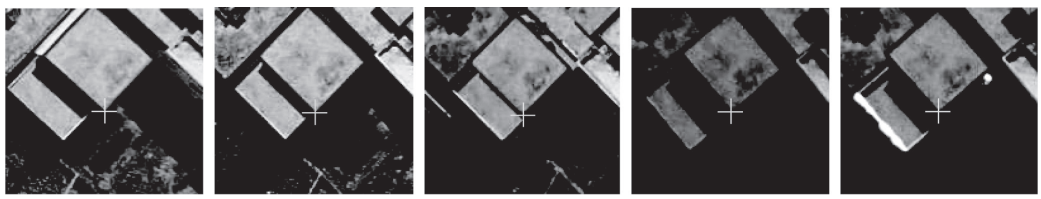

图9 某LiDAR角特征在5张影像上的像点

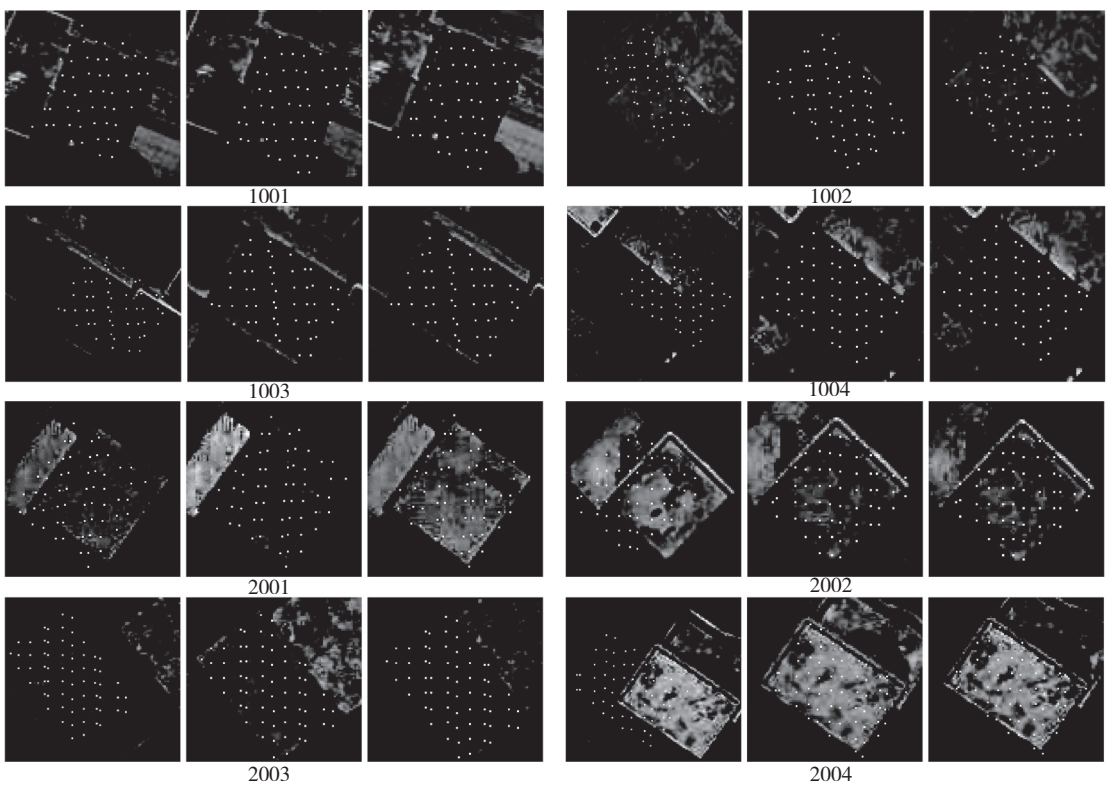

图10 配准前后的效果对比

(每一组图像内左、中、右分别为配准前、采用强度图配准和采用角特征配准后的效果)

表1 配准前后检查点残差对比/m

点名	配准前残差				基于强度图配准后残差				基于角特征配准后残差			
	dX	*dY*	*dXY*	*dZ*	*dX*	*dY*	*dXY*	*dZ*	*dX*	*dY*	*dXY*	*dZ*
A_1	0.38	–0.10	0.39	–2.47	0.05	0.15	0.16	–0.49	–0.07	–0.14	0.16	–0.15
A_2	–1.25	–0.49	1.34	–0.09	0.34	0.06	0.34	–0.11	0.20	–0.06	0.21	0.13
A_3	–0.02	–1.08	1.08	–4.78	0.16	0.06	0.17	–0.12	0.06	–0.12	0.13	0.19
A_4	–0.40	–0.10	0.42	–1.79	0.27	0.24	0.37	–0.29	0.05	0.13	0.14	–0.01
A_5	–1.27	–0.47	1.36	–0.03	0.34	0.16	0.38	–0.20	0.20	0.04	0.20	0.01
A_6	–0.89	0.11	0.89	0.51	0.17	0.27	0.32	–0.21	0.02	0.14	0.14	–0.10
A_7	–0.34	1.02	1.07	2.39	0.28	0.48	0.55	0.03	0.13	0.35	0.37	0.24
A_8	–0.74	0.59	0.95	1.60	–0.15	0.43	0.45	–0.04	–0.32	0.30	0.44	0.08
A_9	–0.58	–0.09	0.59	0.92	0.27	0.30	0.40	–0.14	0.11	0.20	0.23	0.08
残差中误差	0.76	0.58	0.96	2.15	0.24	0.28	0.37	0.23	0.16	0.19	0.25	0.13
残差平均值	–0.57	–0.07	0.90	–0.42	0.19	0.24	0.35	–0.18	0.04	0.09	0.22	0.05
残差最大值	–1.27	–1.08	1.36	–4.78	0.34	0.48	0.55	–0.49	–0.32	0.35	0.44	0.24

配准效果。在LiDAR点云中截取建筑物屋顶点云，然后将屋顶点云根据影像外方位元素投影到影像上(图中白色的点表示投影的屋顶点)，每一组图片的左边为采用初始的影像外方位元素投影的结果，中间为基于强度图配准后的结果，右边为本文提出的基于建筑物角特征配准后的结果。从图中可以看出，左边影像上的屋顶投影点与屋顶的实际位置存在着较大的错位，而经过配准后，在中间和右边影像上套合精度均得到很大的改善，且右边影像上的套合精度优于中间影像上的套合精度。

试验中，在测区内测量了A_1—A_9共9个检查点，表1分别列出了配准前后检查点的平面和高程残差以及各项残差中误差、平均值和最大值，其中*dX*、*dY*、*dZ*分别表示检查点的物方坐标在*X*、*Y*、*Z*方向上的残差，*dXY*为*dX*、*dY*的几何平均值，称为平面残差。从表1的结果可知，配准前检查点在平面、高程方向上的残差中误差分别为0.96 m、2.15 m，最大残差分别为1.36 m、–4.78 m；进行基于强度图的配准后，平面、高程方向上的残差中误差分别为0.37 m、0.23 m，最大残差分别为0.55 m、–0.49 m；进行基于角特征的配准后，平面、高程方向上的残差中误差分别为0.25 m、0.13 m，最大残差降低为0.44 m、0.24 m。鉴于LiDAR数据的点间距约为1.0 m，高程精度约为0.3 m，且影像的地面分辨率约为0.14 m，从表1的结果可知，本文提出的基于建筑物角特征的配准方法达到了理想的配准精度，且其配准精度优于基于强度图的配准方法。

6 结 论

针对城市地区机载LiDAR数据与航空影像集成应用中所面临的数据配准问题，本文提出一种基于建筑物角特征的航空影像与机载LiDAR点云高精度自动配准方法。该方法通过对LiDAR点云构建不规则三角网，从中提取建筑物轮廓线，将轮廓线规则化获得作为配准基元的建筑物角特征。然后采用航空影像初始外方位元素将点云中提取的角特征投影到每张航空影像上，匹配同名的影像角特征。最后将点云和影像间同名角特征的角点作为控制点对航空影像做光束法区域网平差，解求航空影像更准确的外方位元素。并采用循环迭代策略以获取最优配准结果。针对某城市地区的8张航空影像和相应的LiDAR点云数据，分别采用本文提出的基于角特征的配准算法和目前普遍采用的基于点云强度图像的配准算法进行了配准实验，通过对LiDAR屋顶点的投影和检查点残差的分析结果表明本文算法能够得到理想的配准结果，且其配准精度优于基于点云强度图像的配准算法。本文方法的特点如下：(1)不需要将LiDAR点云内插成

图像，避免了点云内插造成的精度损失；(2)采用区域网平差方法，只要整个测区内建筑物数量足够，即使有少数几张影像上因建筑物较少而无法提取控制点，通过区域网平差也能准确解求这些影像的外方位元素，达到航空影像与机载LiDAR点云的整体最佳配准；(3)采用循环迭代策略，在循环过程中可逐步剔除匹配粗差，最终在迭代收敛时获得最优的配准结果。

参考文献(References)

Baltsavias E P. 1999. A comparison between photogrammetry and laser scanning. ISPRS Journal of Photogrammetry and Remote Sensing, 54(2-3): 83–94

程亮, 龚健雅, 李满春, 刘永学, 宋小刚. 2009. 集成多视航空影像与LiDAR数据重建3维建筑物模型. 测绘学报, 38(6): 494–501

邓非, 张祖勋, 张剑清. 2007. 利用激光扫描和数码相机进行古建筑三维重建研究. 测绘科学, 32(2): 29–30

Habib A, Ghanma M, Morgan M and Al-Ruzouq R. 2005. Photogrammetric and lidar data registration using linear features. Photogrammetric Engineering and Remote Sensing, 71(6): 699–707

Habib A F, Shin S, Kim C and Al-Durgham M. 2006. Integration of photogrammetric and LIDAR data in a multi-primitive triangulation environment. [DOI 10.1007/978-3-540-36998-1_3]

Liu X Y, Zhang Z Y, Peterson J and Chandra S. 2007. Lidar-derived high quality ground control information and DEM for image orthorectification. GeoInformatica, 11(1): 37–53

Mastin A, Kepner J and Fisher J. 2009. Automatic registration of lidar and optical images of urban scenes. 2009 IEEE Computer Society Conference on Computer Vision and Pattern Recognition Workshops. Miami Beach: IEEE: 2639–2646

Pothou A, Karamitsos S, Georgopoulos A and Kotsis I. 2006. Assessment and comparison of registration algorithms between aerial images and laser point clouds. Revue Francaise de Photogrammetrie et de Teledetection, (182): 28–33

Shan J and Toth C K. 2008. Topographic Laser Ranging and Scanning: Principles and Processing. Boca Raton: CRC Press: 445–477

沈蔚, 李京, 陈云浩, 邓磊, 彭光雄. 2008. 基于LIDAR数据的建筑轮廓线提取及规则化算法研究. 遥感学报, 12(5): 692–698

Vu T T, Yamazaki F and Matsuoka M. 2009. Multi-scale solution for building extraction from lidar and image data. International Journal of Applied Earth Observation and Geoinformation, 11(4): 281–289

张帆, 黄先锋, 李德仁. 2008. 激光扫描与光学影像数据配准的研究进展. 测绘通报, (2): 7–10

钟成, 李卉, 黄先锋, 李德仁. 2009. 利用6元组松弛法自动配准LiDAR数据与航空影像. 武汉大学学报(信息科学版), 34(12): 1426–1430